

A SURVEY OF BALLISTIC TRANSFERS TO THE LUNAR SURFACE

Rodney L. Anderson* and Jeffrey S. Parker*

In this study techniques are developed which allow an analysis of a range of different types of transfer trajectories from the Earth to the lunar surface. Trajectories ranging from those obtained using the invariant manifolds of unstable orbits to those derived from collision orbits are analyzed. These techniques allow the computation of trajectories encompassing low-energy trajectories as well as more direct transfers. The range of possible trajectory options is summarized, and a broad range of trajectories that exist as a result of the Sun's influence are computed and analyzed. The results are then classified by type, and trades between different measures of cost are discussed.

INTRODUCTION

A wide variety of Earth-Moon trajectories have been employed for past missions ranging from the more direct transfers used for the Apollo missions¹ to more recent missions such as ARTEMIS² that make use of the multi-body dynamics of the Earth-Moon and Sun-Earth-Moon systems. The design of trajectories in multi-body systems is a particularly rich problem because the two-body model is often insufficient to compute accurate trajectories, and the gravity of the Sun, Earth, and Moon combine to form a highly nonlinear dynamical environment. These facts limit the applicability of traditional patched-conic techniques commonly used for interplanetary missions, and the three-dimensional aspects of the problem further complicate real-world missions. Mission designers must take into account the orientation of each body in addition to the relative orientations of the orbits of the Earth and the Moon over time. Parker et al. has studied trajectories that include many of these complicating factors for insertion into a variety of orbit types near the Moon.³⁻⁵ In this study, an analysis including these types of effects is initiated with a focus on trajectories traveling to the lunar surface.

Lunar landing trajectories often have a different set of constraints from those of orbiters, and the nature of this problem makes it possible to approach it with a different set of techniques. Indeed, a theoretical basis for analyzing lunar landing trajectories may be found in the computation of collision orbits. Collision orbits have been studied extensively in the mathematical community by Easton⁶ and McGehee.⁷ Anderson and Lo,⁸ Villac and Scheeres,⁹ and von Kirchbach et al.¹⁰ have previously analyzed collision orbit trajectories for the Jupiter-Europa system and categorized the different regions and trajectories that exist for orbits that terminate or originate at Europa's surface. While the theoretical basis for collision orbits is focused on trajectories that intersect the surface of the selected body normal to the surface, this type of analysis can be extended to trajectories coming in at the various flight path angles and declinations of interest to mission designers. A study of these trajectories is almost directly applicable to impactor missions such as the lunar crater observation and sensing satellite (LCROSS).¹¹ This mission used an 86° impact angle relative to the lunar surface for the impact trajectory. The techniques developed here are also easily applied to systems including the full ephemeris and multiple bodies. Much of the work to design low-energy trajectories from the Earth to the Moon has focused on the use of libration point orbits along with their stable and unstable

*Member of Technical Staff, Jet Propulsion Laboratory, California Institute of Technology, 4800 Oak Grove Drive, M/S 301-121, Pasadena, CA 91109

© 2011 California Institute of Technology. Government sponsorship acknowledged.

manifolds.¹²⁻¹⁵ These techniques have proven to be quite successful, and they are increasingly used for the design of Earth-Moon trajectories. The invariant manifolds of libration orbit trajectories are also briefly studied here with an emphasis on their applicability to landing trajectories.

A wide range of trajectory types for lunar landing trajectories were computed for this study, and presenting a complete picture of the possible trajectory categories while remaining easily accessible was a goal of this research. In keeping with this goal, the problem was approached and presented using several different levels of analysis with increasing complexity, and the paper is structured to parallel this approach. Presenting all different combinations of velocities encountering the surface of the Moon with all different magnitudes and orientations does not allow the relevant structures in the solution space to be easily seen, so two different major divisions were made. In the first, the problem is analyzed for the planar case covering selected velocities or energies with the trajectories encountering the Moon at various angles relative to the surface. The characteristics of these trajectories are observed to lay the groundwork for understanding the spatial trajectory cases, and they are also compared to the invariant manifolds of Lyapunov orbits in the Earth-Moon system. In the second portion of this study, the spatial analysis then focuses on the computation of trajectories encountering the Moon normal to the surface. These trajectories are categorized with the goal of providing a broad survey of the trajectory types that may be available for transfers to the lunar surface from the Earth. The results are placed within the context of results from various sources.¹⁶⁻¹⁸ The specific trades between launch costs and time of flight (TOF) are quantified and summarized in addition to the topological characteristics of the trajectories. Other parameters relevant to mission design such as the launch orientation are computed. The regions of the Moon attainable using different types of trajectories are also characterized. These results are summarized with the goal of providing a tool for mission designers to quickly understand the trades between various measures of cost and time when a particular mission to land on the Moon is being designed.

This study is approached using two key concepts. The first is to view the problem in terms of the limiting bounds that a mission designer could use to refine the search space. This practically takes the form of computing parameters such as the velocities for which trajectories exist that travel from the Earth to the Moon or the launch energies required to reach such trajectories. The second, which is an overall theme of this work and one of the primary results, is related to computationally examining in a more comprehensive sense the trajectories available when the Sun's perturbations are taken into account. To achieve this objective, comparisons involving several different models are made. The questions addressed are directly related to modeling questions¹⁹ and understanding what is necessary to accurately model a system for a given application. Many traditional trajectories were computed using the Earth-Moon model or the circular restricted three-body problem (CRTBP), and in general, similar types of trajectories exist in the full ephemeris model. If simpler models are used, however, some solutions in the full problem may be ignored. Some particular solutions employing the effects of the Sun for transfers in the Earth-Moon system have been examined more recently. The 1991 Japanese mission Muses-A (Hiten) used the effects of the Earth, Moon, and Sun for its transfer to the Moon.²⁰ Koon et al. provided techniques for systematically reproducing missions similar to Hiten using the invariant manifolds of libration orbits.²¹ In each of these techniques the Sun's effects were included in the mission design. Parker and Lo examined trajectories within the Sun-Earth-Moon spatial problem and looked at multiple trajectories for transfer to Lunar halo orbits.^{13,22} The work here seeks to broaden the search space for landing trajectories traveling to the Moon and characterize the effects of the fourth-body perturbations of the Sun on the potential trajectories that may be used. A direct approach isolating the effects of the Sun is taken here by comparing trajectories in the CRTBP, the Earth-Moon system, and the Sun-Earth-Moon system.

MODELS

Two primary models are used for the analyses contained in this study. The first model, the CRTBP, closely approximates real world systems, and a significant set of tools exists within this model to bring to bear on the problem. The qualitative insights gained in this model are very helpful in providing an overview of the categories of trajectories that are available. The trajectories developed within the CRTBP are also generally transferable to the full ephemeris although trajectories developed with the effects of other bodies may not be transferable to the CRTBP. The ephemeris model, implemented using point masses, is used to capture additional types of trajectories that are not found using the CRTBP model. Although the variations in the

orbits of the Earth and Moon are important, this model is primarily used to search for members of the broad category of trajectories utilizing the Sun's perturbation for Earth-Moon transfers.

Circular Restricted Three-Body Problem

The initial analysis performed in this paper is carried out within the CRTBP.²³ In this model, two bodies, typically referred to collectively as the primaries, are placed in circular orbits revolving about their center of mass, and the objective is to describe the motion of a third infinitesimal mass. The equations of motion are usually formulated in a rotating frame so that the x axis is aligned with the primaries. Dimensionless quantities are used so that the larger body (the primary) has mass $1 - \mu$, and the smaller body (the secondary) has mass μ . The distance between the primary and secondary is then unity with the primary located on the x axis at $x_1 = -\mu$ and the secondary at $x_2 = 1 - \mu$. The period of the rotating system is 2π , while the mean motion and the gravitational constant are both unity. The dimensionless time corresponds to the angle between the x axis of the rotating frame and the x axis of the inertial frame. Using this notation, the equations of motion for the infinitesimal mass in the rotating frame may be written as

$$\begin{aligned}\ddot{x} - 2\dot{y} &= \frac{\partial\Omega}{\partial x} \\ \ddot{y} + 2\dot{x} &= \frac{\partial\Omega}{\partial y} \\ \ddot{z} &= \frac{\partial\Omega}{\partial z}\end{aligned}\tag{1}$$

where

$$\Omega = \frac{x^2 + y^2}{2} + \frac{(1 - \mu)}{r_1} + \frac{\mu}{r_2}\tag{2}$$

and

$$\begin{aligned}r_1 &= \sqrt{(x - x_1)^2 + y^2 + z^2} \\ r_2 &= \sqrt{(x - x_2)^2 + y^2 + z^2}.\end{aligned}\tag{3}$$

The Jacobi constant is an energy-like integral defined by

$$C = x^2 + y^2 + \frac{2(1 - \mu)}{r_1} + \frac{2\mu}{r_2} - \dot{x}^2 - \dot{y}^2 - \dot{z}^2\tag{4}$$

that is also known to exist in this problem. There are five equilibrium points in the problem (the Lagrange points) about which periodic orbits may be found. In this study, the collinear Lagrange points (referred to as L_1 , L_2 , and L_3) are situated so that L_1 is between the primary and the secondary, L_2 is on the far side of the secondary from the primary, and L_3 is on the far side of the primary. For particular Jacobi constants there are positions where the resulting velocity is imaginary. A spacecraft cannot travel into these forbidden regions, and the curve bounding them is referred to as a zero velocity curve. The specific parameters used in this study are listed in Table 1.

The existence of symmetries in the CRTBP is of particular interest for this analysis. Miele in his examination of image trajectories in the Earth-Moon space noted that one of these symmetries allows Moon-Earth trajectories to be computed from Earth-Moon trajectories. Specifically, he showed that if $(x, y, z, \dot{x}, \dot{y}, \dot{z}, t)$ is a solution in the CRTBP, then $(x, -y, z, -\dot{x}, \dot{y}, -\dot{z}, -t)$ is also a solution. In other words, if a trajectory is reflected about the xz plane, a valid trajectory is obtained by traveling along the reflected trajectory in reverse. This property eliminates the need to compute approach and departure trajectories separately in the CRTBP, and a similar effect would be expected in the real world. Again, see Szebehely for a more detailed description of this property.

Ephemeris Model

While the CRTBP provides advantages in that it is well understood and provides a close approximation to the Earth-Moon system, mission designers ultimately compute real-world trajectories traveling to or from the

Table 1. Constants used in the CRTBP and this analysis.

Quantity	Value
GM_{Earth} (km ³ /s ²)	398600.43623333969
GM_{Moon} (km ³ /s ²)	4902.80007622774
μ	0.012150584270572
Radius _{Earth} (km)	1737.40
Radius _{Moon} (km)	6378.14
Period _{Moon} (sec.)	2360591.5104
Geosynchronous Radius (km)	42164.17

Moon within the full ephemeris. In the full ephemeris the eccentricity and orientation of the Moon's orbit must be taken into account in addition to perturbations from other bodies such as the Sun. The Moon's mean eccentricity is 0.05490, and its mean inclination relative to the ecliptic is 5.145396 degrees.²⁴ Rather than remaining constant as in the CRTBP, the distance from the Earth to the Moon varies from its mean distance of approximately 3.844×10^5 km.²⁴ Using these parameters, the distance from the Earth to the Moon varies from roughly 363296.44 km to 405503.56 km. In general a form of most of the trajectories computed within the CRTBP can be computed in the ephemeris model, but these trajectories may require that the Moon be in a particular point in its orbit. A notable difference in the two models is due to the influence of the Sun, which as mentioned before, may sometimes be taken advantage of to reduce the overall required ΔV to travel to the Moon. The influence of the sun and other effects are examined here using the JPL DE421 Planetary and Lunar Ephemerides.²⁵ For more detailed information on lunar physical constants and geometry within the context of the JPL Lunar Ephemeris 403, see Roncoli.²⁶

BOUNDS ON THE PROBLEM

In analyzing trajectories traveling to the lunar surface, it is useful to first examine the dynamics of the system in the CRTBP before jumping to the ephemeris problem. The CRTBP accurately captures the general characteristics of the system, and it can provide a convenient tool for early mission design before specific mission details are known. Comparisons with results obtained using the full ephemeris can then provide insight into the potential benefits or drawbacks of modeling the actual orbits and perturbing bodies more accurately.

One of the initial questions to address when looking at transfers to the lunar surface involves determining bounds on the velocities or energies needed to reach the surface of the Moon from the Earth. Several general bounds exist that limit the movement of a spacecraft in the CRTBP. Using knowledge of the forbidden regions, it is known that a trajectory is not able to travel between the Earth and the Moon if it has a Jacobi constant value above that of the value at the L_1 libration point. It is unable to travel from the Earth-Moon region to the exterior region until the Jacobi constant decreases below that of the L_2 lagrange point. Remember that decreasing the Jacobi constant corresponds to increasing energy or velocity, which can be seen by referring back to Equation 4. The Jacobi constants of the libration points are listed next for comparison with the values shown in subsequent plots.

$$\begin{aligned}
 C_{L_1} &= 3.1883411054012485 \\
 C_{L_2} &= 3.1721604503998044 \\
 C_{L_3} &= 3.0121471493422489 \\
 C_{L_4}, C_{L_5} &= 2.9879970524275450
 \end{aligned} \tag{5}$$

Sweetser computes a lower bound of 3.721 km/s on the ΔV to travel from a 167 km altitude circular orbit at the Earth to a 100 km altitude circular orbit at the Moon in the CRTBP.¹⁶ Actual trajectories have been computed that approach this theoretical minimum in the CRTBP,¹⁸ but it is here that incorporating the perturbations of the Sun become important in reducing costs to below this CRTBP theoretical minimum.

Additional bounds on the problem may be obtained by computing relevant dynamical structures for each energy level. These include libration orbits and their invariant manifolds. It is well known that libration orbits act as a gateway through which trajectories transiting between different regions at certain energies in the CRTBP must pass.^{27,28} The computation of the invariant manifolds can act as guides for potential trajectory pathways in the Earth-Moon system.

Despite the existence of these bounds on the trajectory design space, the number of remaining Earth-Moon trajectories continues to be infinite. It is here that the practical consideration of TOF can be introduced to limit the scope of the problem. Collision orbits terminating at the surface of the Moon may be computed and analyzed in a systematic manner to determine which ones provide an acceptable pathway to the Earth. The problem may be further expanded to include orbits with non-perpendicular intersections with the Moon's surface, and the potential design space of lunar landing trajectories is then canvassed. It is limited only by the granularity of the grid of the computed trajectories terminating at the Moon's surface and the selection of the model for the system. This approach is taken for this study, and unless otherwise indicated, the integration time period for the presented trajectories is taken to have a maximum of 200 days. It is also worth noting again that for each trajectory approaching the Moon from the Earth in the CRTBP there exists a trajectory reflected about the xz plane that returns to the Earth. It is expected that similar trajectories will also exist in the ephemeris problem, so this study can be used to provide an analysis of Earth-return trajectories using this technique.

PLANAR ANALYSIS

The procedure described above involves varying the location of the landing site on the Moon, the orientation of the incoming trajectory, and the energy/velocity of the trajectory. Each trajectory must then be characterized or evaluated using some figure of merit. While this can provide a relatively complete picture of the potential trajectory options, it is helpful to first gain insight into the dynamics by limiting the scope of the problem to allow the results to be easily visualized.

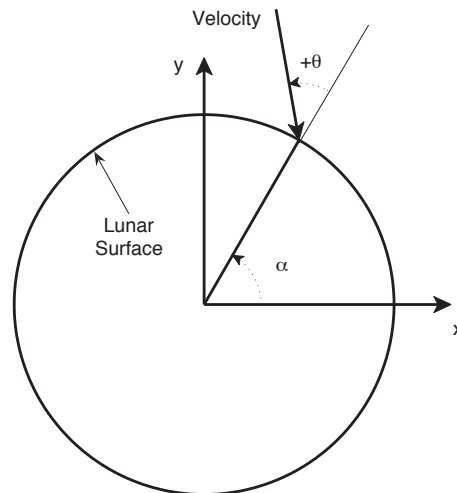


Figure 1. Diagram showing location and orientation of velocity vector as it intersects the lunar surface. The xy axes shown here are centered on the Moon in the same orientation as the axes in the rotating frame.

Several different techniques have been used to achieve this goal in the Jupiter-Europa system, and it is useful to consider their application here. One technique used in Anderson and Lo⁸ varied the Jacobi constant for trajectories intersecting Europa on a sphere for several different trajectory orientations and characterized the origin of the trajectories. Kirchbach et al.¹⁰ examined the planar case for the Jupiter-Europa system for additional velocity orientations leaving the surface. Both of these techniques are applied here to the Earth-

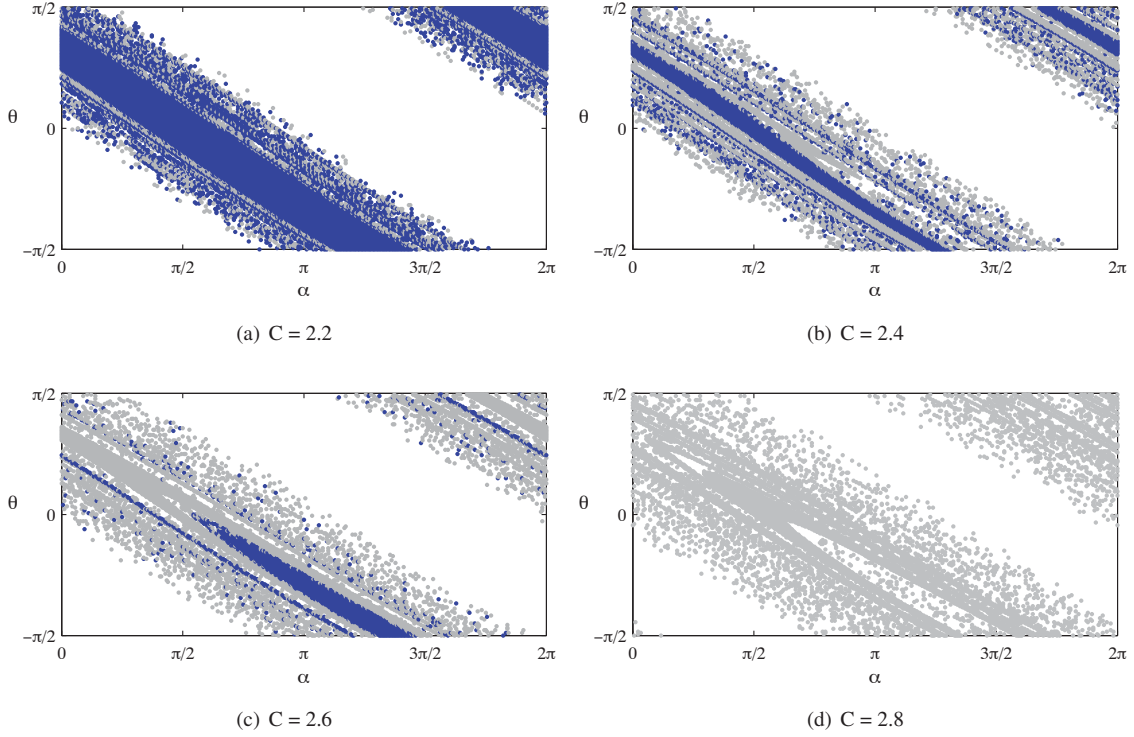


Figure 2. Plots showing the origin of each trajectory as a function of the position and orientation of the velocity vectors as the trajectories encounter the Moon’s surface. Blue points indicate that the trajectory originated at the Earth and gray that it originated at the Moon. If no point is plotted the integrated trajectory did not encounter the surface of either body over the given time span of 200 days. (Earth-Moon CRTBP)

Moon system, and it is interesting to start with the planar problem in order to gain some initial insight. First, the planar results are computed in the Earth-Moon CRTBP system to allow for a comparison with the results from Kirchbach et al. in the Jupiter-Europa system. This technique is then used to extend the analysis to the ephemeris case with the Earth and Moon and then to the case where the Sun is included. The effect of adding the Sun is examined in detail over a range of Jacobi constants.

For this planar analysis, a set of trajectories was integrated backward in time from the surface of the Moon. Specifying the Jacobi constant gives the velocity magnitude for each trajectory, while the location of the trajectory and the orientation of the velocity are specified using α and θ as shown in Figure 1. Multiple simulations were performed using these techniques, and the results for several selected Jacobi constant values are given in Figure 2. The resulting points are colored according to the original location of each trajectory. Note that if a trajectory integrated backward in time were to intersect the Moon and then encounter the Earth at an earlier time, the trajectory would be gray. The (α, θ) point corresponding to the intermediate intersection of the Moon would then be blue. The fact that points with only slightly different initial conditions in the plot can travel to either the Earth or the Moon confirms the known existence of chaos in this problem. Comparison with the results from the Jupiter-Europa system in Kirchbach et al. reveals that the dividing lines between different regimes of motion are less distinct at equivalent Jacobi constants for the Earth-Moon system. This existence of chaos indicates that it may be possible to design trajectories that cover a relatively wide range of the surface by carefully selecting landing sites. It is useful to note here again that Moon-Earth transfers may be derived from Earth-Moon transfers, and the plot corresponding to these trajectories may be obtained from Figure 2 for the planar problem using $x \rightarrow x, y \rightarrow -y, \dot{x} \rightarrow -\dot{x}$, and $\dot{y} \rightarrow \dot{y}$. The transformation in position gives $\alpha \rightarrow 2\pi - \alpha$ and then from examination of the transformed velocity vector, $\theta \rightarrow -\theta$.

As can also be seen from the results, a significant percentage of the trajectories do not encounter either the primary or the secondary over the given time span. However, it is useful to note that for low Jacobi constants (higher energies) a significant percentage of the trajectories do originate at the Earth. Determining the Jacobi constant where Earth-Moon transfer trajectories no longer exist in the planar problem can help provide a rough limit on energies or velocities for these trajectories and provide a method for determining the potential benefits of perturbations from other bodies in trajectory design. To determine the approximate Jacobi constant above which Earth-Moon trajectories computed in this simulation no longer exist, a series of runs were made in parallel to step through the Jacobi constant. The grid resolution used for this step was one degree in both α and θ . The percent of the total number of trajectories that encountered the Earth for each Jacobi constant was computed and plotted in Figure 3. As expected from the previous plots, the number of trajectories originating at the Earth generally decreases with increasing Jacobi constant, but it is interesting that the slope of the curve varies significantly over the plotted range. It is also interesting that although the curve approaches zero percent near a Jacobi constant of 2.7, for Jacobi constants as high as 2.78 the percent of trajectories originating at the Earth remains at approximately 0.03 percent or approximately 19 trajectories. So even for this relatively low energy some trajectories manage to travel from the Earth to the Moon.

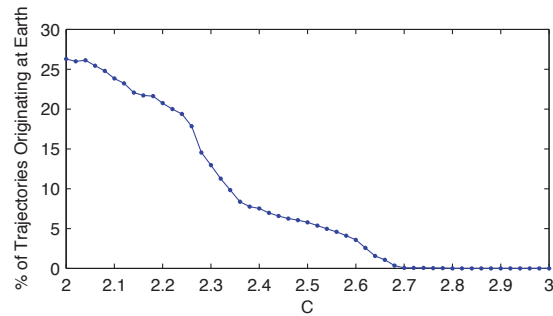


Figure 3. Percent of trajectories originating at the Earth for each Jacobi constant (CRTBP).

For mission design, it is helpful to be aware of the velocities of the trajectories as they intersect the surface. They will actually vary somewhat as the constant for the computations so far has been the Jacobi constant rather than velocity. In general the inertial velocities relative to the Moon only vary at the m/s level. Figure 4 shows the average velocities for the case with velocities normal to the surface as a reference for each Jacobi constant.

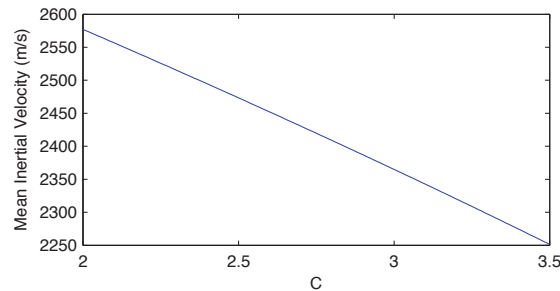


Figure 4. Mean inertial velocities relative to the Moon at each Jacobi constant for the cases with velocities normal to the surface.

Although the CRTBP is known to provide an accurate approximation to real world trajectories, an obvious question for mission designers is related to how much the inclusion of real world effects would affect selected trajectories. This question can be addressed by using planetary ephemerides and replicating the analysis for the CRTBP in this model. This analysis was first performed in the ephemeris model initially including only

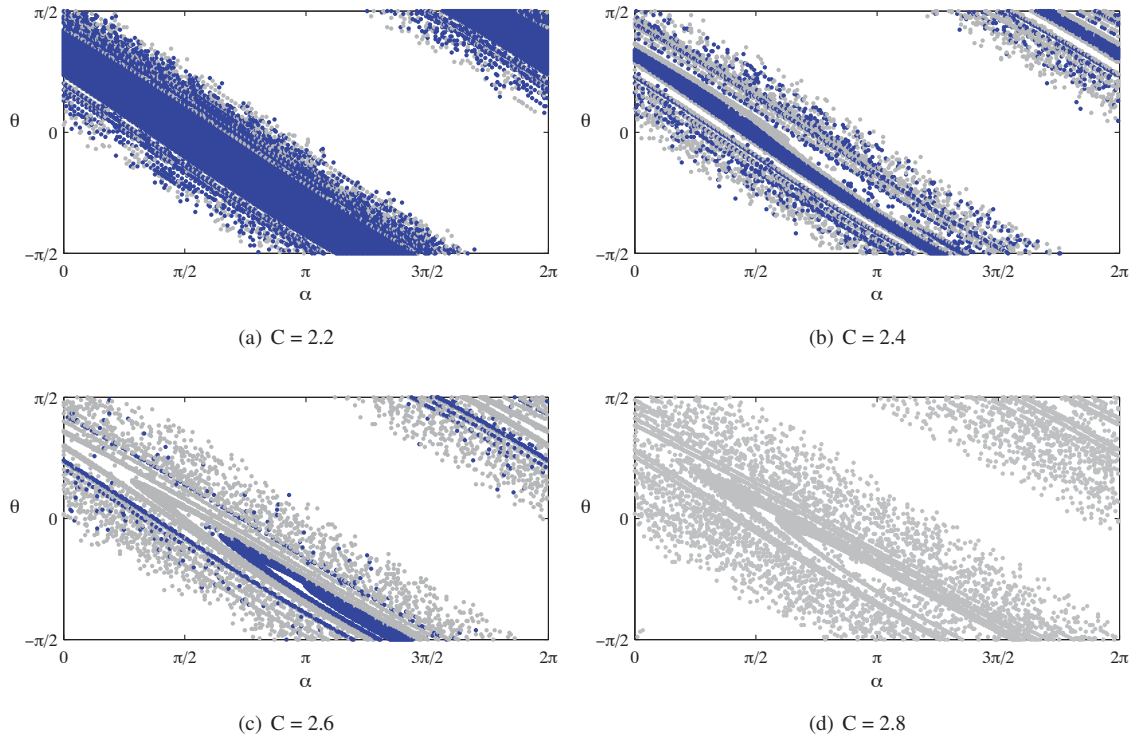


Figure 5. Plots showing the origin of each trajectory as a function of the position and orientation of the velocity vectors as the trajectories encounter the Moon. Blue points indicate that the trajectory originated at the Earth and gray that it originated at the Moon. If no point is plotted the integrated trajectory did not encounter either body over the given time span of 200 days. (Earth-Moon only Ephemeris System)

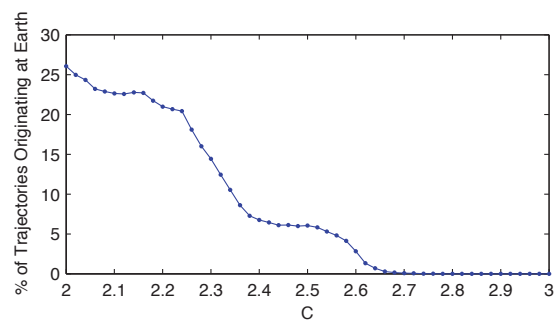


Figure 6. Percent of trajectories originating at the Earth for each Jacobi constant (Earth-Moon only Ephemeris System).

the gravity of the Earth and Moon. The initial velocities were computed for a given Jacobi constant in the CRTBP in the rotating frame, and then the states were initialized in the integrator relative to the Moon in an instantaneous rotating frame aligned with the Earth-Moon frame on an epoch of January 1, 2015. As the distance between the Earth and the Moon varies over the course of the orbit, it is difficult to obtain a direct comparison to the results from the CRTBP, but this method was selected because it was found to provide a good approximate comparison. The initial conditions were initially planar, but the trajectory was free to vary in three dimensions for this problem. Using this method for a system including the Earth and Moon ephemerides, the trajectories were integrated, and the results are plotted in Figure 5. Comparing the results

for this system with the results in Figure 2 reveals few obvious differences. The Earth impacting cases for $C = 2.6$ have some slight differences, but in general the trajectories match the expectation that the CRTBP is a good approximation to the three-body problem including the ephemerides. If the percent of trajectories originating at the Earth are compared, some differences in the shape of the curve can be found, but the overall trends are very similar. In this case, the percent of trajectories in Figure 6 originating at the Earth decreases down to 0.006 percent at $C = 2.76$, approximately the same Jacobi constant cutoff as the CRTBP.

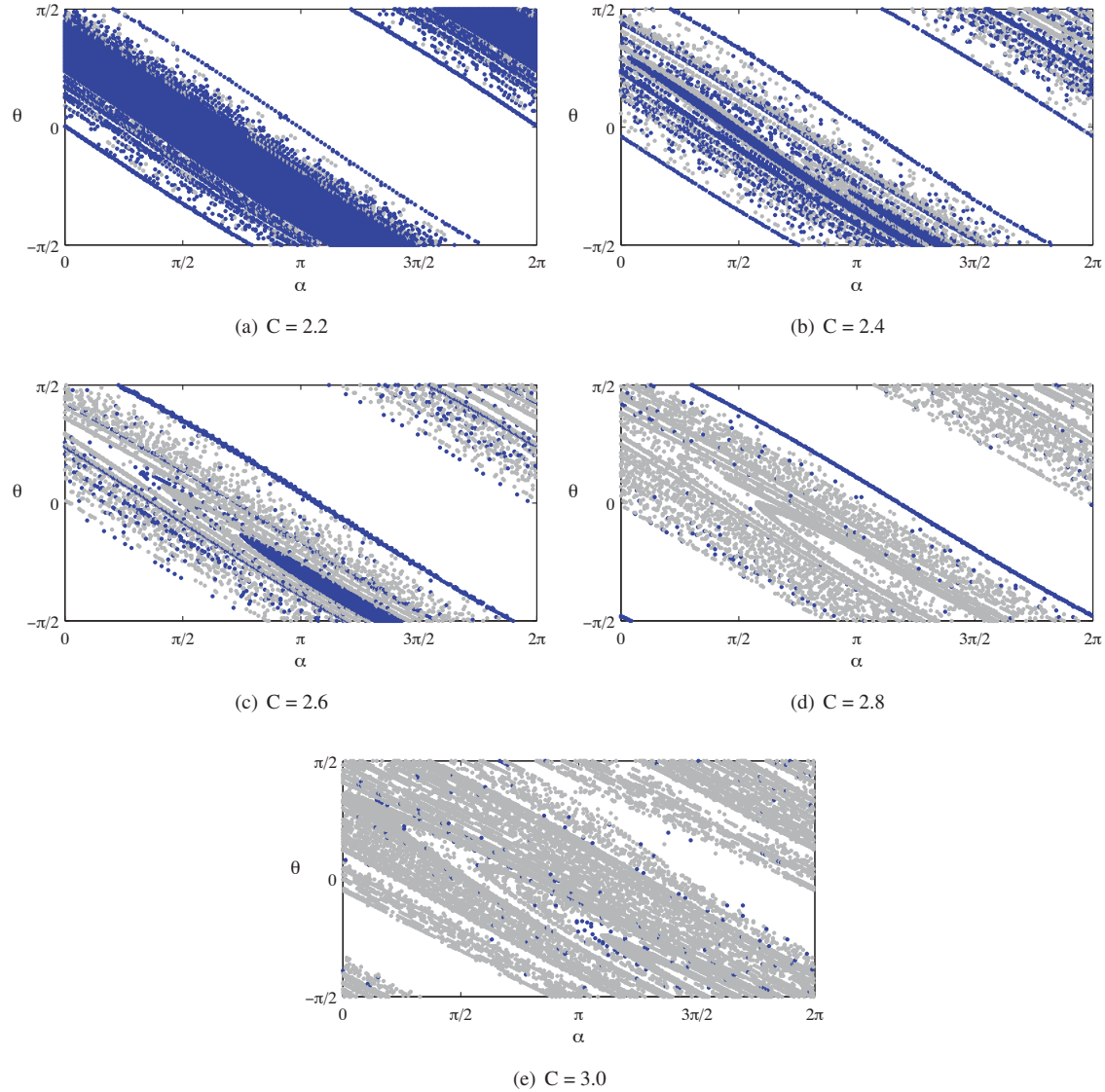


Figure 7. Plots showing the origin of each trajectory as a function of the position and orientation of the velocity vectors as the trajectories encounter the Moon. Blue points indicate that the trajectory originated at the Earth and gray that it originated at the Moon. If no point is plotted the integrated trajectory did not encounter either body over the given time span of 200 days. (Sun-Earth-Moon Ephemeris System)

Next, the same procedure was performed including the Sun in the integration, and the results are plotted in Figure 7. Now, comparison with the results in both the CRTBP and the Earth-Moon systems reveal some obvious differences. Several new bands of trajectories originating at the Earth spring into existence. The

overall structure remains generally similar, but the points appear chaotic. A new band of solutions remains for $C = 2.8$ and a significant number of Earth origin trajectories still exist at $C = 3.0$. If the percent of trajectories originating at the Earth is examined in Figure 8(a), it can be seen that at $C = 3.0$, 0.3 percent of the trajectories still originate at the Earth. Indeed, as high as $C = 3.16$, 0.15 percent of the trajectories still originate at Earth. One immediate question that arises is whether the selected epoch for lunar arrival would significantly affect these results, so three additional cases seven days apart were computed and plotted in Figure 8(b). Some variation is observed as the Moon travels through its orbit with one case starting with

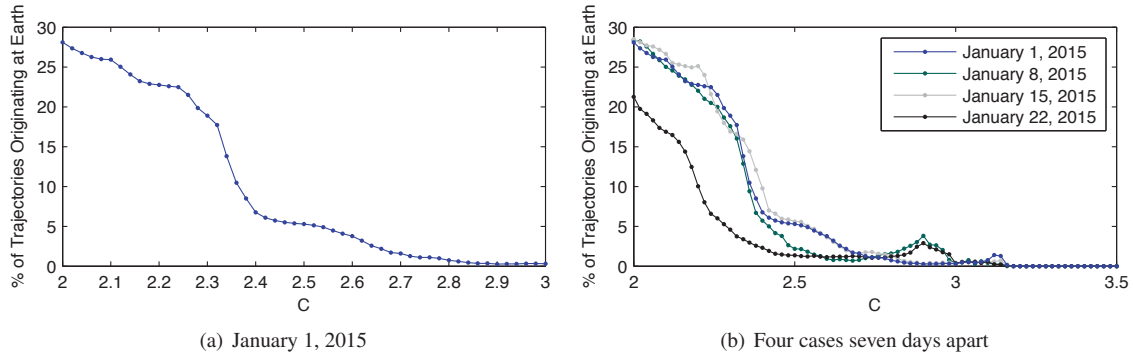


Figure 8. Percent of trajectories originating at the Earth for each Jacobi constant (Sun-Earth-Moon Ephemeris System).

a lower percent of trajectories for low Jacobi constants and two of them possessing peaks just before $C = 3.0$. However, all of them have approximately the same upper Jacobi constant cutoff of approximately $C = 3.16$ where the percent of trajectories drops to near zero. The existence of the additional bands of trajectories and the increase in the Jacobi constant where trajectories connecting the Earth and Moon exist in this system raises the question as to where these trajectories come from. These trajectories were plotted in both the Earth-Moon system and the Sun-Earth-Moon system to examine the differences, and a sample of one of these trajectories plotted in both rotating frames is given in Figure 9. As can be seen from the plots, the trajectory ends up in very different places depending on whether the Sun is included in the integration or not. In the Earth-Moon rotating frame with the Sun included, the trajectory travels far away from the system with no close periapses until it approaches the Earth, while the case without the Sun has two relatively close periapses at approximately the lunar distance and ends up far from the Earth. The most telling plots, however, are in the Sun-Earth rotating frame. Here, the characteristic shape of a trajectory using the libration point dynamics of the Sun-Earth system is apparent when the Sun is included. The trajectory travels out toward the L_1 point, lingers there, and then finally falls back toward the Earth. Without the Sun, the trajectory stays out near the Moon until it eventually wanders further away from the system, unless there is a lunar flyby.

Manifolds

The use of invariant manifolds for transfers has become increasingly common in trajectory design, and it is helpful to understand the energies at which the manifolds intersect the lunar surface. The simplest trajectories to use for this computation are planar Lyapunov orbits in the planar CRTBP, so they are analyzed here to obtain an estimate of the Jacobi constants where the manifolds just encounter the surface of the Moon. Further analysis of these types of trajectories will be performed for additional orbits and spatial or three-dimensional cases in a future paper. The invariant manifolds for the L_1 and L_2 Lyapunov orbits when the manifolds are just tangent to the surface are plotted in Figure 10. The Jacobi constant for the L_1 manifold case is higher as expected, and it corresponds to an inertial velocity relative to the Moon of approximately 2298 m/s. The L_2 manifold case produces an inertial velocity relative to the Moon at the surface of 2330 m/s.

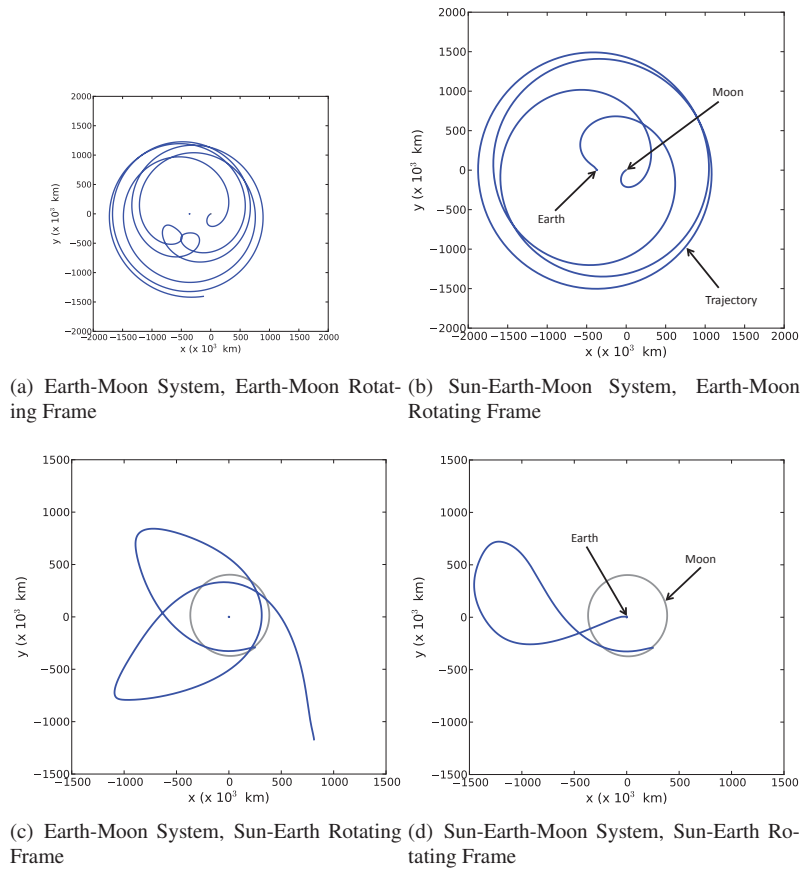


Figure 9. Comparison of a single trajectory at $C = 2.8$ ($\alpha \approx 197.5^\circ$, $\theta \approx 9.5^\circ$) integrated with and without the Sun's gravity in different rotating frames.

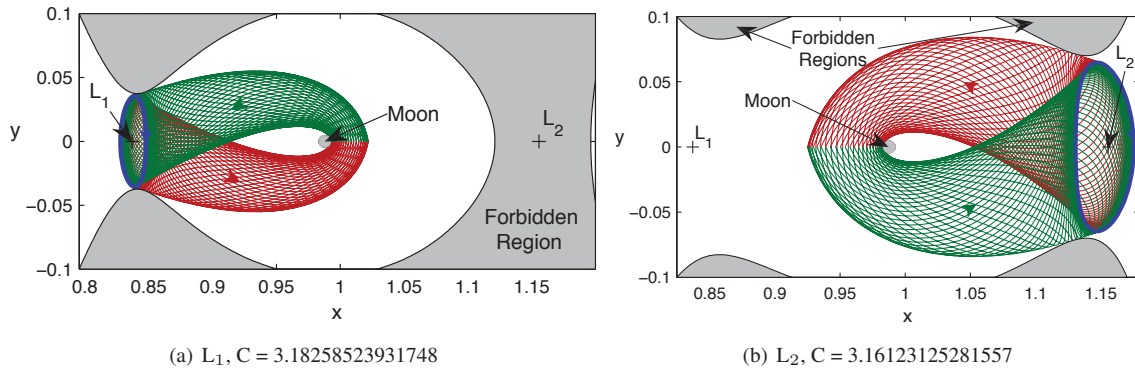


Figure 10. Manifolds of libration orbits at Jacobi constants where the manifolds just begin to reach the surface of the Moon.

SPATIAL ANALYSIS

While the planar cases discussed up to this point are quite complicated, it is still possible to plot many of the salient features of the design space given the relatively small dimension of the problem. With the increase in dimension that occurs for the spatial problem, the visualization of the resulting trajectories and

their characteristics becomes an even more difficult issue. One of the stated objectives of this analysis is to capture the characteristics of the major trajectory categories while also providing adequate information to evaluate the usefulness of each trajectory. With this objective in mind it is worth noting that if the plots in Figures 2, 5, and 7 are examined it can be seen that the majority of the dominant types of trajectories seen in the figures may be captured by making a particular cut at $\theta = 0$. The trajectories obtained with $\theta = 0$ correspond to those trajectories impacting the Moon normal to the lunar surface. As previously mentioned, these types of trajectories are particularly applicable to impactor missions similar to LCROSS. Given the results from the planar case, they can also provide a good initial overview of the different categories of Earth-Moon landing trajectories including those with different flight path angles. The results presented next are restricted to those computed using impacts normal to the surface. They provide accurate results for impactor-type trajectories, and they also give a good indication of the types of trajectories that may exist for trajectories coming in at other flight path angles.

To allow for easy visualization of the trajectory characteristics, the results are presented for each energy level, which corresponds to a slightly varying velocity magnitude relative to the Moon depending on the location of the final point on the trajectory at the Moon's surface. The velocity can be used to provide an indication of the ΔV required for landing, although the specific ΔV will depend on the particular landing trajectory. The regions of the Moon that are accessible for each energy level can be evaluated for particular mission design requirements by using the desired parameters plotted over the surface of the Moon in α and ϕ . α and ϕ are measured in the rotating frame with α positive in the same direction as shown in Figure 1. ϕ is measured like latitude and is positive above the xy plane. Understanding how to connect the trajectory to the Earth becomes more of a challenge in the spatial problem because a large number of possible Earth-relative orientations and methods of injection onto the trans-lunar trajectory are possible. For this reason, a specific set of trajectory characteristics were selected for plotting. The procedure in each case was to begin with the final point on the trajectory with a velocity normal to the lunar surface at the given α and ϕ . The trajectory was then propagated backward in time until it either encountered the Earth or the Moon, or the trajectory duration reached 200 days. For those trajectories not encountering the Earth or the Moon in this time period, a search was then made for the periaipse closest to the Earth. Several quantities were then computed using the point at encounter or periaipse. They included the periaipse radius relative to the Earth, the TOF, the launch energy (C_3), and inclination in the Earth mean equator frame (EME2000).

Results showing the origin of each trajectory encountering the Moon are given in Figure 11. For these cases three-dimensional effects are included, and it is now possible for the trajectory to miss encounters with the Earth and Moon by traveling above or below them. A significant number of encounters are still observed though, and the features seen for the $\theta = 0$ cases in the planar model may still be observed here where ϕ is 0° . Although a significant number of Earth origin trajectories are observed for low Jacobi constants, as the Jacobi constant increases (energy decreases), the number of Earth-Moon transfers decreases. Once a Jacobi constant of 2.8 is reached, there are no more of these types of trajectories in the Earth-Moon system model. However, there are still a significant number of Earth-Moon trajectories in the model including the Earth, Moon, and Sun. Indeed, a significant number still exist as the Jacobi constant is increased even above 3.1. This observation emphasizes the need to include the Sun's influence in the trajectory design process, but it raises the question as to what types of Earth-Moon trajectories exist at these energies, and how long are their time of flights? It is difficult to answer these questions completely since trajectories are constantly changing with energy, but it is interesting to observe some of the trajectories that exist in the Sun-Earth-Moon system with no corollary in the Earth-Moon system. Two sample trajectories from the line of Earth origin trajectories at $C = 2.6$ that do not exist in the Earth-Moon system are given in Figure 12. The majority of cases found in this line are similar to the trajectory in Figure 12(a), and they exhibit the characteristics of known trajectories designed to utilize the dynamics of the invariant manifolds of libration orbits. They approach the L_1 Lagrange point from the Earth in the Sun-Earth system and then fall away toward the Moon. Although almost all of the trajectories follow this type of orbit, some do have characteristics similar to the trajectory in Figure 12(b). In this case, the Sun's gravity is still influential, but an intermediate flyby is inserted.

It is also interesting to observe the types of trajectories that exist for higher Jacobi constants in the Sun-Earth-Moon system where no analogues in the Earth-Moon system have been found. Several samples are

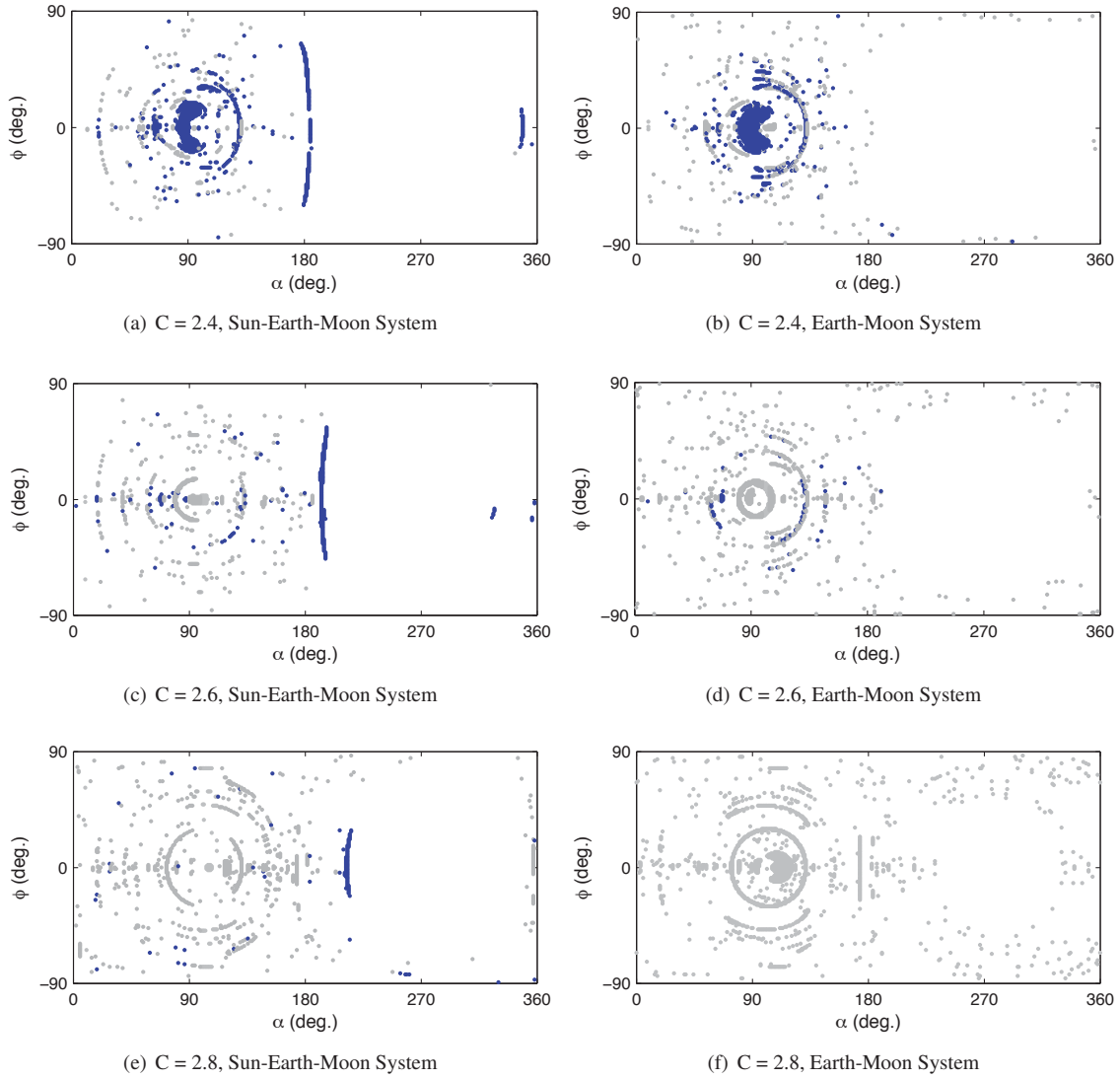


Figure 11. Plots showing the origin of the spatial collision trajectories. Blue indicates the trajectory originated at the Earth, and gray indicates it originated at the Moon. If it is white, no encounter occurred within 200 days.

shown along with the trajectory origin plots in Figure 13 to provide an overview of these types of trajectories. Here, an interesting phenomenon occurs. As the Jacobi constant increases to 3.0, the trajectories originating at the Earth are scattered across the map. The majority of the Earth-origin trajectories seem to require multiple flybys of the Earth or the Moon. The sample trajectories shown in Figure 13(a) are intended to be representative of the types of trajectories found across the map. Although a few trajectories, such as those found in the lower left corner of the map, utilize the libration dynamics more directly, the majority seem to require variations on different phasing flybys as shown by the various trajectories. As the Jacobi constant is increased further to a value of 3.1 in Figure 13(b), a line of trajectories appear. These trajectories, as shown in the figure, once again utilize the libration orbit dynamics more directly, sometimes making use of a single flyby along the trajectory. The remaining scattered trajectories found near the center of the plot continue to use multiple gravity flybys to connect the Earth and the Moon.

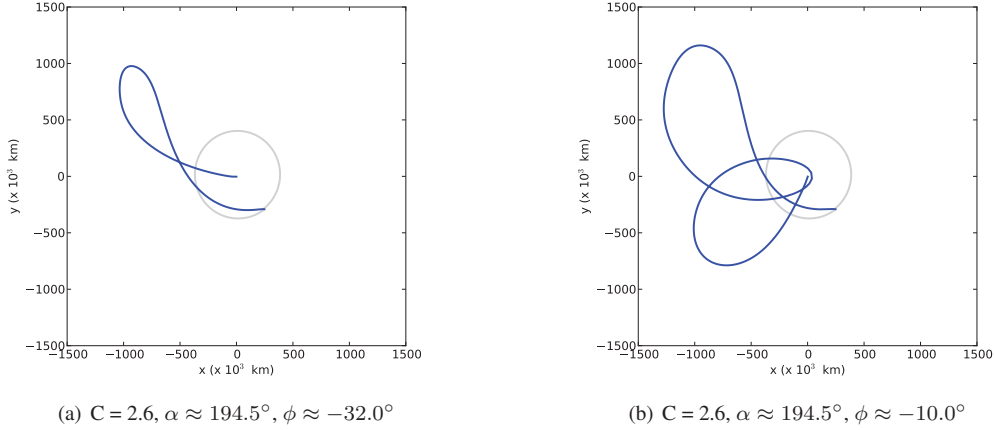


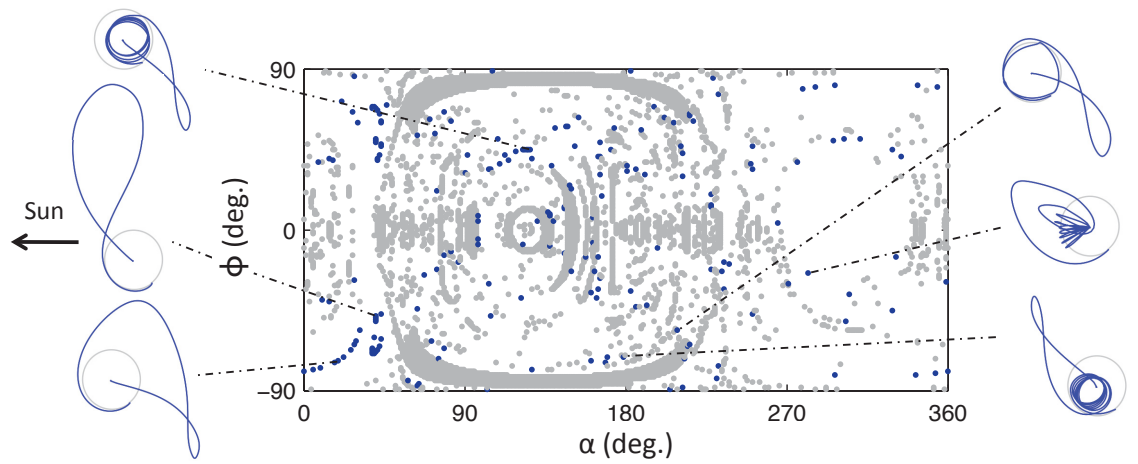
Figure 12. Sample trajectories at $C = 2.6$ for the Sun-Earth-Moon system. The trajectories correspond to the line of trajectories not found in the Earth-Moon plots.

Another interesting characteristic to include in the analysis is the TOF required for each trajectory originating at the Earth. More specifically, what are the minimum TOF values that may be achieved at each energy? The TOF values provide an indication of whether the trajectories at each Jacobi constant fall more in the category of direct transfers, low-energy transfers, or somewhere in between. The existence of trajectories in the Sun-Earth-Moon system that do not exist in the Earth-Moon system already indicates the presence of trajectories utilizing multi-body effects that would be expected to fall more in the low-energy category. The minimum TOF values for selected Jacobi constants are listed in Table 2. These values were computed using a grid with the points spaced at one degree intervals in each variable. As expected, the TOFs start near the

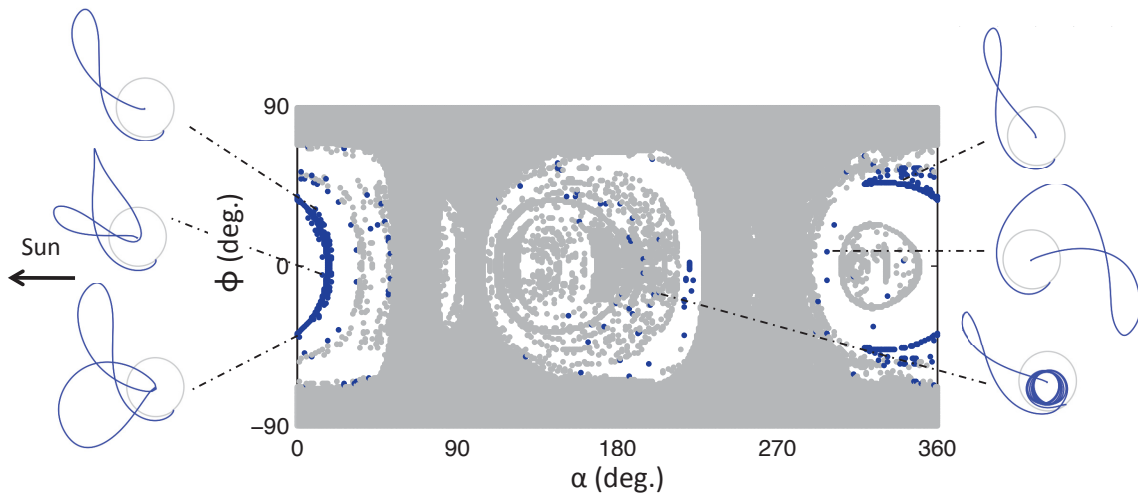
Table 2. Minimum TOF values from the computed trajectories originating at the Earth for selected Jacobi constants.

C	TOF (days)
2.2	3.4
2.4	29.8
2.6	58.3
2.7	57.8
2.8	74.0
2.9	94.9
3.0	101.0
3.1	78.7

three day values seen for the Apollo program's direct transfers for a Jacobi constant of 2.2, and climb to over 100 days for a Jacobi constant of 3.0. It is surprising though that the minimum TOF at a Jacobi constant of 3.1 drops to 78.7 days. Although this point is lower than most of the others at this energy, a number of trajectories still exist in the 90 day time range. The reasons behind this drop in the TOF may be more clearly understood by reexamining the typical trajectories plotted for the Jacobi constants of 3.0 and 3.1 in Figure 13. As mentioned previously, the majority of the trajectories computed for the Jacobi constant of 3.0 required multiple phasing flybys, while the $C = 3.1$ trajectories typically utilize the libration dynamics without these phasing loops. This phenomenon would explain the lower minimum TOF value at $C = 3.1$, since many of the trajectories at this energy actually use a more direct approach.



(a) $C = 3.0$, Sun-Earth-Moon System



(b) $C = 3.1$, Sun-Earth-Moon System

Figure 13. Plots showing the origin of the spatial collision trajectories. Blue indicates the trajectory originated at the Earth, and gray indicates it originated at the Moon. If it is white, no impact occurred within 200 days. Trajectories are shown for select points in the Earth-centered Sun-Earth rotating frame. The gray circular orbit is the Moon's orbit while the Sun is in the indicated direction. The scale is the same for all trajectories shown, and the trajectories all originate at the Earth.

The analysis so far has focused on categories of trajectories originating at the Earth with the expectation that trajectories from a given category may often be modified to meet the particular requirements of a mission when they are supplied. Often, however, trajectories that originate within some distance of the Earth may be used by targeting them from low Earth orbit. It is also important to quantify the orbital parameters of the initial conditions of the analyzed trajectories relative to the Earth in order to determine the suitability of the trajectories for particular missions. For example, if a launch from Cape Canaveral is selected, an inclination relative to the Earth's pole of 28.5° would be desirable. Particular quantities relevant to mission design are presented next with the objective of presenting an overview of the possible trajectories so that initial estimates may be made for future mission design. The analysis here focuses on the Sun-Earth-Moon system so as to encompass the complete range of trajectories.

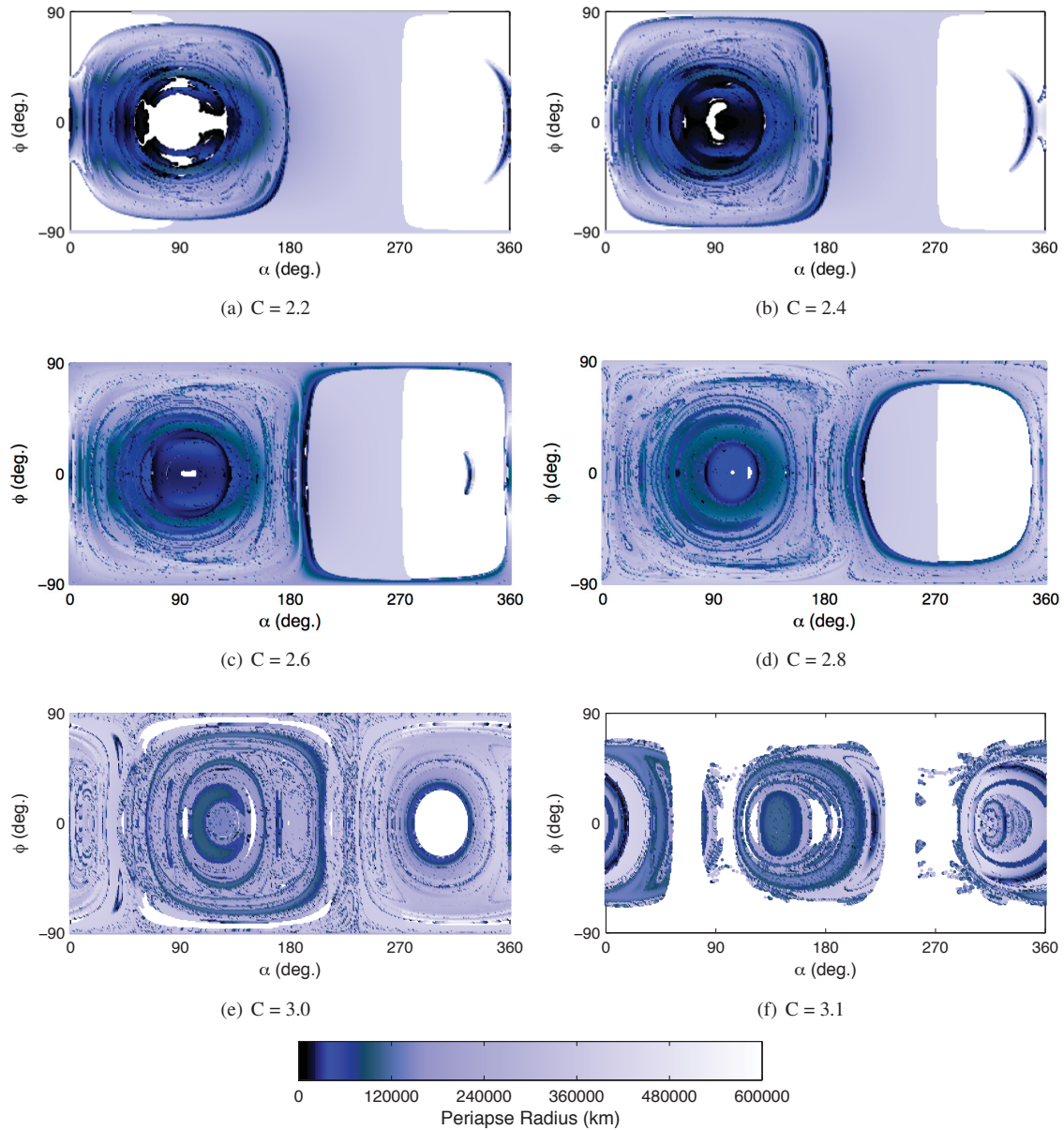


Figure 14. Periaapse radius values for the computed trajectories plotted over the surface for a range of Jacobi constant values.

The closest periaapse values obtained over 200 days for selected Jacobi constants in the Sun-Earth-Moon system are plotted in Figure 14. Note that some of the gaps in (a) are Earth intersection trajectories as can be seen by reexamining Figure 13. It can immediately be seen from the plots that the majority of the trajectories never come near the Earth. In general, the trajectories originating near $\alpha = 90^\circ$ produce the most trajectories with periaapses closer to Earth. This does shift with Jacobi constant as was seen in the earlier Europa study.⁸ As the Jacobi constant increases and energy decreases, it appears that fewer trajectories come as close to the Earth, but the majority stay near the system. The chaos present in the system can especially be observed for $C = 3.0$ where trajectories very close to each other alternate with low and high periaapses. It appears that a large portion of the lunar surface may be physically accessible to trajectories coming from the Earth, but the feasibility of flying these trajectories will depend on parameters in Figures 15 and 16 such as TOF, launch

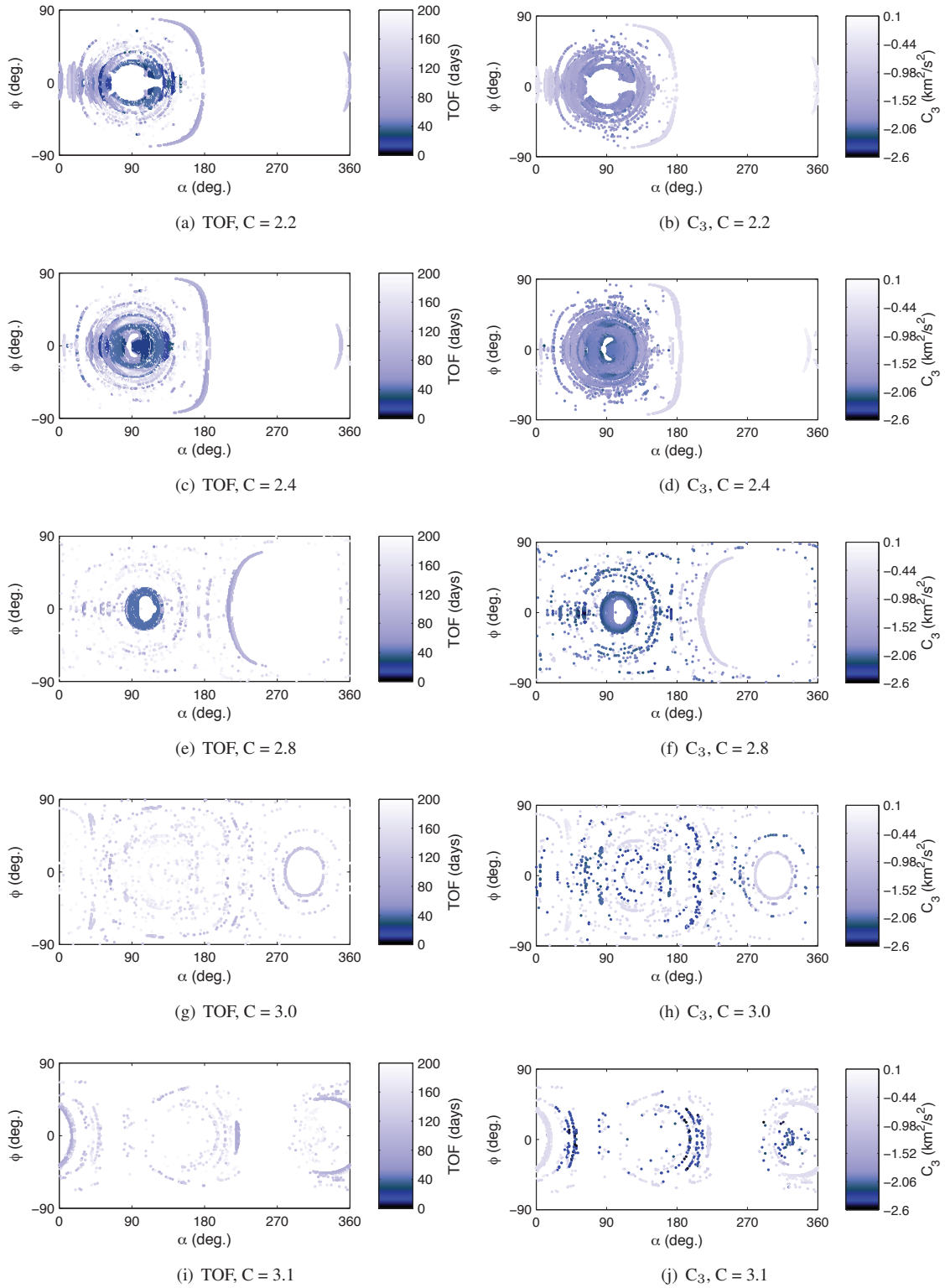


Figure 15. TOF and C_3 for each trajectory plotted over the surface for a range of Jacobi constants.

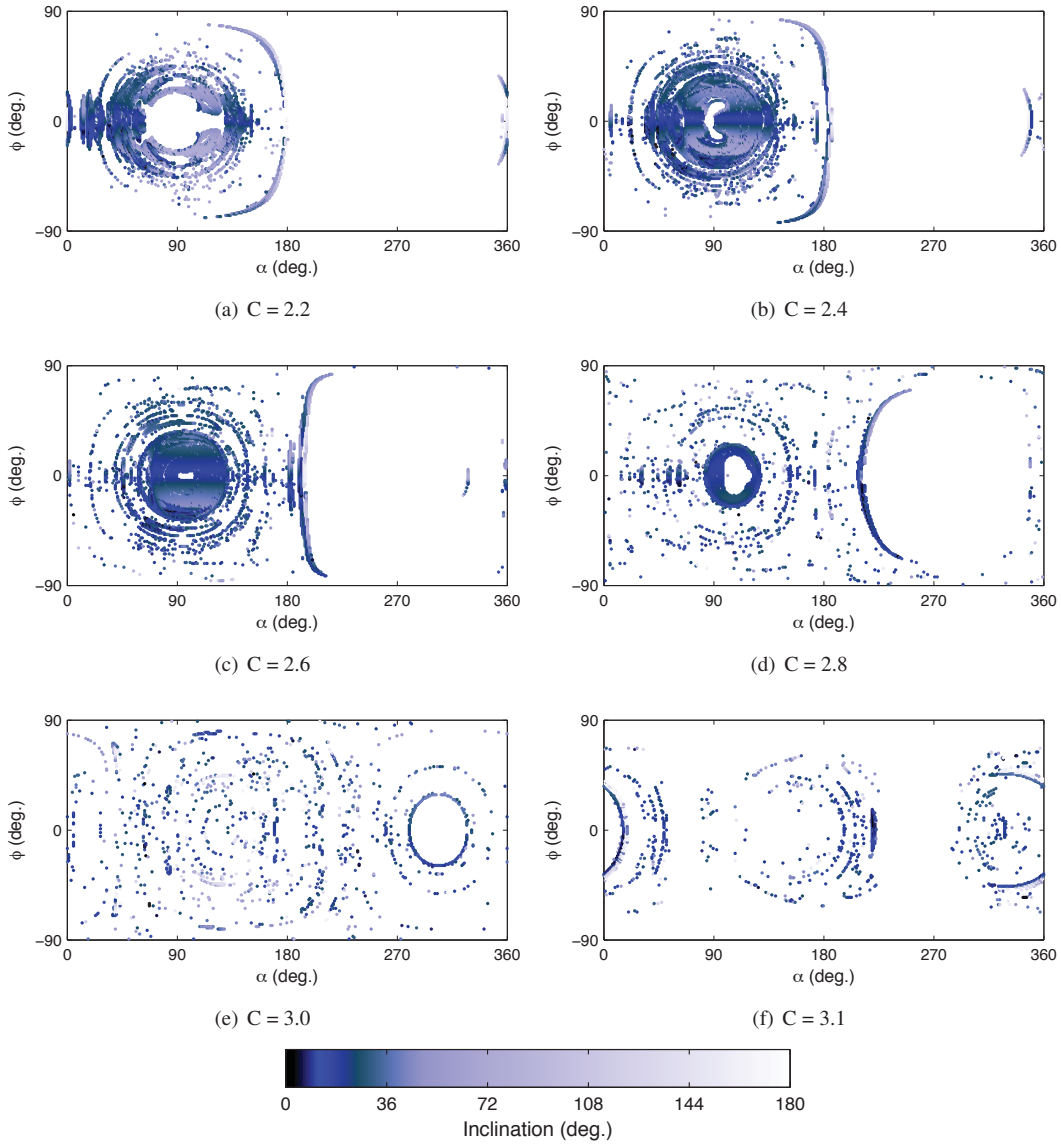


Figure 16. Inclination computed relative to the Earth in the EME2000 coordinate frame.

energy (C_3), and inclination. It is uncertain what a two-body orbital element parameter means when it is computed where multi-body perturbations are significant. So only parameters for trajectories with periapses lower than geosynchronous radius are plotted in the following figures. For these plots, the parameters are now included for those trajectories originating at the Earth, and in those cases their values are computed using the initial conditions at the Earth's surface.

The TOFs and C_3 values are plotted in Figure 15 for those trajectories with periaxis relative to the Earth of less than geosynchronous radius. The immediate feature that can be noticed is the sparsity of points compared to the previous plots, confirming that a large number of trajectories ending at the lunar surface never come near the Earth. Indeed, for lower Jacobi constants, the locations between approximately 180° and 360° have almost no trajectories originating near the Earth. Curiously, around a Jacobi constant of 3.0, the trajectories are more randomly distributed across the surface with a combination of C_3 values. This feature may be partly explained by returning to the TOF values. From the plots, it can be confirmed that the minimum

TOFs generally increase with Jacobi constant. The minimum TOF values at $C = 3.0$ are significantly larger, indicating that low-energy trajectories under the influence of chaos are beginning to be more common. Given the variety of trajectory types and the TOFs involved, it is not surprising that more of the lunar surface is potentially covered. Examining the trends in the TOF plots, it may also be observed that longer TOF trajectories appear to exist at each energy level. The lines of long TOF trajectories correspond to low-energy trajectories using the Sun's perturbations and approaching the libration points of the Sun-Earth system. It is also worth noting that a variety of C_3 options are available at each energy level for transfers to the Moon. Even for low Jacobi constants, there still exist some relatively low C_3 options, although the minimum is higher than that found for the higher Jacobi constant cases. It is important to realize that a small change in the landing location can result in a drastic change in the required C_3 even with similar TOFs and the same velocity at the Moon. This fact is important for mission designers as it may sometimes be possible to move the landing site slightly to improve ΔV , or a similar effect may be obtained by targeting with maneuvers along the trajectory. Trajectory correction maneuvers may also help aid in reducing the ΔV . In general, it is useful to be aware of the chaotic nature of the design space as seen from these plots.

Finally, it is important for most mission designs to consider the inclination. The inclination results in the EME2000 coordinate frame are given in Figure 16. One of the important features to notice here is that a variety of inclinations are possible. A choice of trajectories exist with the lower inclinations suitable for launch from Cape Canaveral. The particular inclinations needed for a mission will depend on the target location on the Moon and the particular constraints of the mission. They are provided here as a sample of the range of the values that are possible.

CONCLUSIONS

A broad range of trajectories traveling from Earth to the lunar surface have been surveyed in the CRTBP, the Earth-Moon ephemeris model, and the Sun-Earth-Moon ephemeris model. The CRTBP modeled the most important aspects of the Earth-Moon system when the Sun's perturbations were not included. Adding the Sun into the ephemeris model was shown to have a significant effect on the overall set of solutions, producing more solutions with lower velocities. One of the primary results of this paper is that a statistically significant set of trajectories exist for lunar landing trajectories as a result of the Sun's perturbation that would not exist without it. This builds on the specific solutions that have been discovered in earlier works, and makes the case for further exploration of these types of trajectories. Specific characteristics of the Earth-Moon landing trajectories were explored including the Sun's effects, and the results were presented for use in mission design. The existence of trajectories that can go from the Earth with acceptable orientations while still covering a significant portion of the lunar surface was shown. The low-energy category of trajectories allows for a wider exploration or coverage of the lunar surface, and the chaotic nature of these trajectories emphasizes the need for careful design. It also provides the opportunity to find low ΔV trajectories given the proper selection of parameters and landing sites.

FUTURE WORK

Some remaining areas for future work, some of which have already been initiated, include analyzing the potential trajectories over a wider range of different dates. They also include a fuller analysis of all potential trajectories with different flight path angles at the Moon in three dimensions. Manifolds were briefly touched on here, and a detailed survey of the use of invariant manifolds for lunar landing is planned in the future.

ACKNOWLEDGEMENTS

The research presented in this paper has been carried out at the Jet Propulsion Laboratory, California Institute of Technology, under a contract with the National Aeronautics and Space Administration.

REFERENCES

- [1] Mission Evaluation Team, "Apollo 11 Mission Report," Tech. Rep. NASA SP-238, National Aeronautics and Space Administration, 1971.

- [2] S. B. Broschart, M.-K. J. Chung, S. J. Hatch, J. H. Ma, T. H. Sweetser, S. S. Weinstein-Weiss, and V. Angelopoulos, "Preliminary Trajectory Design for the ARTEMIS Lunar Mission," *AAS/AIAA Astrodynamics Specialist Conference*, No. AAS 09-382, Pittsburgh, Pennsylvania, August 10-13 2009.
- [3] J. S. Parker, "Low-Energy Ballistic Transfers to Lunar Halo Orbits," *AAS/AIAA Astrodynamics Conference*, No. AAS 09-443, Pittsburgh, Pennsylvania, August 9-13 2009.
- [4] J. S. Parker, "Monthly Variations of Low-Energy Ballistic Transfers to Lunar Halo Orbits," *AIAA/AAS Astrodynamics Specialist Conference*, No. AIAA 2010-7963, Toronto, Ontario, Canada, August 2-5 2010.
- [5] J. S. Parker, "Targeting Low-Energy Ballistic Lunar Transfers," *George H. Born Symposium*, No. AAS, Boulder, Colorado, May 13-14 2010.
- [6] R. W. Easton, "Regularization of Vector Fields by Surgery," *Journal of Differential Equations*, Vol. 10, 1971, pp. 92-99.
- [7] R. McGehee, "Triple Collision in the Collinear Three-Body Problem," *Inventiones Mathematicae*, Vol. 27, 1974, pp. 191-227.
- [8] R. L. Anderson and M. W. Lo, "Virtual Exploration by Computing Global Families of Trajectories with Supercomputers," *AAS/AIAA Space Flight Mechanics Conference*, No. Paper AAS 05-220, Copper Mountain, Colorado, January 23-27 2005.
- [9] B. F. Villac and D. J. Scheeres, "Escaping Trajectories in the Hill Three-Body Problem and Applications," *Journal of Guidance, Control, and Dynamics*, Vol. 26, March-April 2003, pp. 224-232.
- [10] C. v. Kirchbach, H. Zheng, J. Aristoff, J. Kavanagh, B. F. Villac, and M. W. Lo, "Trajectories Leaving a Sphere in the Restricted Three Body Problem," *AAS/AIAA Space Flight Mechanics Meeting*, No. AAS Paper 05-221, Copper Mountain, Colorado, January 23-27 2005.
- [11] D. S. Cooley, K. F. Galal, K. Berry, L. Janes, G. Marr, J. Carrico, and C. Ocampo, "Mission Design for the Lunar CRater Observation and Sensing Satellite (LCROSS)," *AIAA/AAS Astrodynamics Specialist Conference*, No. AIAA-2010-8386, Toronto, Ontario, Canada, August 2-5 2010.
- [12] M. W. Lo and M.-K. J. Chung, "Lunar Sample Return via the Interplanetary Superhighway," *AIAA/AAS Astrodynamics Specialist Meeting*, No. Paper AIAA 2002-4718, Monterey, California, 2002.
- [13] J. S. Parker and M. W. Lo, "Shoot the Moon 3D," *AAS/AIAA Astrodynamics Specialist Conference*, No. Paper AAS 05-383, Lake Tahoe, California, August 7-11 2005.
- [14] J. S. Parker, "Families of Low-Energy Lunar Halo Transfers," *AAS/AIAA Space Flight Mechanics Conference*, No. Paper AAS 06-132, Tampa, Florida, January 22-26 2006.
- [15] M. Ozimek and K. Howell, "Low-Thrust Transfers in the Earth-Moon System Including Applications to Libration Point Orbits," *Journal of Guidance, Control, and Dynamics*, Vol. 33, March-April 2010.
- [16] T. H. Sweetser, "Estimate of the Global Minimum DV Needed for Earth-Moon Transfer," *AIAA/AAS Spaceflight Mechanics Meeting*, No. 91-101, Houston, TX, February 1991.
- [17] T. H. Sweetser, "Several Ways to Leave for Luna," *AAS/AIAA Astrodynamics Specialist Conference*, No. Paper AAS 95-402, Halifax, Nova Scotia, Canada, August 14-17 1995.
- [18] H. J. Pernicka, D. P. Scarberry, S. M. Marsh, and T. H. Sweetser, "A Search for Low ΔV Earth-to-Moon Trajectories," *The Journal of the Astronautical Sciences*, Vol. 43, January-March 1995, pp. 77-88.
- [19] R. Barzel, *Physically-Based Modeling for Computer Graphics: A Structured Approach*. Boston, Massachusetts: Academic Press, 1992.
- [20] E. A. Belbruno and J. K. Miller, "Sun-Perturbed Earth-to-Moon Transfers with Ballistic Capture," *Journal of Guidance, Control, and Dynamics*, Vol. 16, July-August 1993, pp. 770-774.
- [21] W. S. Koon, M. W. Lo, J. E. Marsden, and S. D. Ross, "Low Energy Transfer to the Moon," *Celestial Mechanics and Dynamical Astronomy*, Vol. 81, 2001, pp. 63-73.
- [22] J. S. Parker, *Low-Energy Ballistic Lunar Transfers*. PhD thesis, University of Colorado at Boulder, Boulder, Colorado, 2007.
- [23] V. Szebehely, *Theory of Orbits: The Restricted Problem of Three Bodies*. New York: Academic Press, 1967, pp. 7-41.
- [24] P. K. Seidelmann, ed., *Explanatory Supplement to the Astronomical Almanac*. Sausalito, California: University Science Books, 1992.
- [25] W. M. Folkner, J. G. Williams, and D. H. Boggs, "The Planetary and Lunar Ephemeris DE421," Interoffice Memo IOM 343R-08-003, Jet Propulsion Laboratory, March 31 2008.
- [26] R. B. Roncoli, "Lunar Constants and Models Document," Tech. Rep. JPL D-32296, Jet Propulsion Laboratory, September 23 2005.
- [27] C. Conley, "Low Energy Transit Orbits in the Restricted Three-Body Problem," *SIAM Journal of Applied Mathematics*, Vol. 16, 1968, pp. 732-746.
- [28] R. P. McGehee, *Some Homoclinic Orbits for the Restricted Three Body Problem*. PhD thesis, University of Wisconsin, Madison, Wisconsin, 1969.